Final Draft
of the original manuscript:

Lin, R.; Betten, J.; Brocks, W.:
Modeling of finite strain viscoplasticity based on the logarithmic corotational description
In: Archive of Applied Mechanics (2006) Springer

DOI: 10.1007/s00419-006-0044-6

Modeling of finite strain viscoplasticity based on the logarithmic corotational description

R.C. Lin[1,3], J. Betten[2] and W. Brocks[1]

[1]*Institute of Materials Research, GKSS Research Center, Max-Planck-Str. 1, D-21502 Geesthacht, Germany*

[2]*Mathematical Models in Materials Science and Continuum Mechanics, Technical University Aachen, Augustinerbach 4-22, D-52064 Aachen, Germany*

[3]*Institute of Engineering Strucutre & Mechanics, Dalian Maritime University, 116026 Dalian, China*

Abstract

It has been proven that the deformation rate is identical to the logarithmic corotational rate of the spatial logarithmic strain. Based on the logarithmic corotational description we present an extension of a Chaboche's infinitesimal viscoplastic law for finite strain cases. An additive decomposition of the logarithmic corotational rate of the logarithmic strain, implicitly included in an internal dissipation inequality, is applied for the extension. Functionally, this additive decomposition corresponds to the additive decomposition of the material derivative of the logarithmic strain used in infinitesimal inelastic problems. Using the additive decomposition and replacing the material time derivatives of all second-order tensors in the infinitesimal viscoplastic law with the corresponding logarithmic corotational rates we arrive at a new finite viscoplastic law with nonlinear isotropic and kinematic hardening. The numerical algorithms suitable for the finite element implementation of this law are formulated and several numerical examples are presented. These numerical examples prove that the finite viscoplastic law and the algorithms are effective and reliable.

Keywords

Viscoplasticity, logarithmic corotational rate, internal dissipation

1. Introduction

A lot of metals deforms viscoplastically, particularly at elevated temperatures. In order to describe the viscoplastic behavior many constitutive laws have been developed. The representatives are Chaboche's viscoplastic laws, see e.g. Chaboche [11, 12, 13, 14, 15], Chaboche and Jung [16], Chaboche and Rousselier [17, 18] as well as Lemaitre and Chaboche [21]. Many applications have proven that the Chaboche viscoplastic laws can characterize constitutive responses of many metals very well, see e.g. Chaboche [12] and Lemaitre and Chaboche [21]. But, almost all of the Chaboche laws are mathematically formulated in the context of infinitesimal deformations. This infinitesimal condition hinders the application of these laws to problems with finite deformations, for example, to simulation of metal forming processes and description of mechanical responses of metal structures at finite deformations. In order to exploit the advantages of the Chaboche laws for finite deformation problems it is necessary to reformulate the classical Chaboche laws for finite deformation cases. At the formulation of a finite viscoplastic law an important task is to choose suitable objective rates for the viscoplastic evolution equations.

In the context of infinitesimal deformations the local deformation variation rate at a point is described by the time derivative of the strain tensor at that point. But, in the context of finite deformations this variation rate usually is measured by the deformation rate tensor. Both rate measures play similar roles in their corresponding deformation contexts. In the spatially described finite inelastic theories, the deformation rate tensor is often applied. But, the application of the material time derivatives of spatial strain and deformation tensors is limited by the objective principle of material. In the past decade, it was proven that the deformation rate tensor is essentially identical to the logarithmic corotational rate of the spatial logarithmic strain [20, 37, 38]. At infinitesimal deformations this objective rate reduces to the material time derivative of the strain automatically. In recent years, an internal dissipation inequality, with the Kirchhoff stress and the difference of the logarithmic corotational rates of the total and elastic logarithmic strains being the dissipation-conjugate pair, was presented and applied to the viscoelastic and mixed viscoelastic-elastoplastic characterizations of polymers and elastomers by Lin [22] and Lin and Schomburg [25]. The

viscoplastic and elastoplastic laws based on this dissipation inequality have been compared with other corresponding inelastic laws based on other three dissipation inequality by Lin et al. [27]. The mathematical structure of this dissipation inequality implies a kinematic assumption: the additive decomposition of the logarithmic corotational rate of the total logarithmic strain into an elastic and an inelastic part. This additive decomposition reduces automatically to the additive decomposition of the time derivative of the total strain at infinitesimal deformations. The latter additive decomposition is widely applied in infinitesimal inelastic theories. It can be easily seen that the above arguments support the selection of the logarithmic corotational descriptions of spatial objective rates for finite inelastic laws. Of course, there are also other formulations of spatial objective rates. In fact, many finite inelastic theories are based on conventional objective rates and hypoelastic laws. This type of formulation is also extensively applied in the commercial general-purpose finite element programs, for example in ABAQUS [2]. By this approach, one can also reformulate the Chaboche laws for finite strain cases. But, it has been shown that the hypoelastic equations related to the conventional stress rates are not consistent with elasticity and cause spurious constitutive responses in deformation processes with finite rotations [23, 24]. The reason for these spurious responses is that the types of these conventional stress rates are different from the type of the spatial deformation rate, which is a logarithmic corotational rate of the spatial logarithmic strain. Simo and Pister [36] suggested that the hypoelastic formulation should be replaced by the hyperelastic formulation for establishing a finite strain inelastic law. In recent years several finite strain plastic and viscoplastic theories based on the latter formulation have been presented. See, for example, the works of Simo [32], Simo and Miehe [35] as well as Miehe [29]. Other two types of internal dissipation inequalities described in the corotational coordinate system rotated by the polar rotation tensor and in the intermediate unloaded configuration have been also applied to finite inelastic constitutive formulations [26, 28].

In the present contribution we formulate a new finite viscoplastic law using the logarithmic corotational description and based on an Chaboche's infinitesimal viscoplastic law. The elastic constitutive relation is expressed in the hyperelastic form. For clarity and as a reference, the infinitesimal viscoplastic law is summarized first. After showing some necessary basic aspects of continuum mechanics we present the internal dissipation using the logarithmic corotational

description. Based on this inequality the infinitesimal viscoplastic law is then extended for finite strain cases. The numerical algorithms for finite element implementation of the finite viscoplastic law are formulated in Section 4. Several numerical examples are presented in Section 5 to prove the correctness and effectivity of the theoretical formulations and numerical algorithms. The paper is concluded with Section 6.

2. A Chaboche viscoplastic law at small deformations

To motivate the extension of the Chaboche viscoplastic law to finite strain form it is summarized in this section. This summary stems mainly from the works presented in Chaboche [13, 14], Chaboche and Jung [16], Lemaitre and Chaboche [21]. See also Arzt et al. [3]. This viscoplastic law is based on the phenomenological Bingham model (see Fig. 1). It can be easily seen that the plastic unit and the viscous unit correspond to a unique inelastic strain. In the viscoplastic laws based on this phenomenological model the effects related to two types of inelastic deformations, e.g. the hardening due to deformation (strain-hardening) and the hardening due to time (time-hardening), are usually treated in combined ways. In this sense this class of viscoplastic laws is usually called *unified* viscoplastic law.

The following additive decomposition of total strain $\boldsymbol{\varepsilon}$ is assumed, i.e.

$$\boldsymbol{\varepsilon} = \boldsymbol{\varepsilon}^e + \boldsymbol{\varepsilon}^p, \tag{1}$$

where $\boldsymbol{\varepsilon}^e$ is the linear elastic strain and $\boldsymbol{\varepsilon}^p$ is the viscoplastic strain. This additive decomposition is consistent with the experimental observation that for most metals the elastic behavior is not affected by the magnitude of viscoplastic strain. The total strain is specified by the partial derivative of

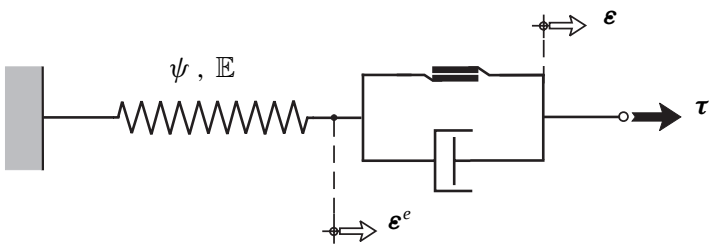

Fig. 1: Bingham phenomenological model

displacement $\boldsymbol{u}$ with respect to spatial position vector $\boldsymbol{x}$; i.e. $\boldsymbol{\varepsilon} = \frac{1}{2}\left[\frac{\partial \boldsymbol{u}}{\partial \boldsymbol{x}} + (\frac{\partial \boldsymbol{u}}{\partial \boldsymbol{x}})^{\mathrm{T}}\right]$. In general, both the elastic strain and the viscoplastic strain can be considered as internal variables. But, only one of them is independent because of equation (1). In this viscoplastic law the viscoplastic strain is chosen as an independent internal variables. Isotropic and kinematic hardening are included. In order to treat both types of hardening two strain-like internal variables: the scalar p and the second-order strain-like tensor $\boldsymbol{\xi}$ are introduced. The former is used to characterize isotropic hardening and can be chosen, as a specific case, as $p = \varepsilon^p = \int_0^t \left(\frac{2}{3}\dot{\boldsymbol{\varepsilon}}^p : \dot{\boldsymbol{\varepsilon}}^p\right)^{1/2} \mathrm{d}\tau$, with ε^p being the accumulated plastic strain. The latter is assumed to be work-conjugate to a stress-like internal variable: the back stress $\boldsymbol{\alpha}$ and is used to characterize kinematic hardening.

In this constitutive theory it is assumed that there are two types of potential functions: the free energy function Ψ described in the strain space and the dissipation potential function Φ described in the stress space. Further, the free energy (per unit reference volume) is assumed to be decoupled and is formulated as (see e.g. Lemaitre and Chaboche [21], p. 312)

$$\Psi = \psi_e(\boldsymbol{\varepsilon}^e) + g(\boldsymbol{\xi}) + \ h(p), \tag{2}$$

where ψ_e and g are the elastic free energy and the kinematic hardening function defined respectively as

$$\psi_e(\boldsymbol{\varepsilon}^e) = \tfrac{1}{2}\,\boldsymbol{\varepsilon}^e : \mathbb{C} : \boldsymbol{\varepsilon}^e, \qquad g(\boldsymbol{\xi}) = \tfrac{1}{3} C\,\boldsymbol{\xi} : \boldsymbol{\xi}\,. \tag{3}$$

Here, $\mathbb{C}$ is an isotropic fourth-order elastic tensor defined by $\mathbb{C} = \lambda \mathbf{1} \otimes \mathbf{1} + 2\mu\mathbb{I}$ or expressed in index notation [9, 10] as $\mathbb{C}_{ijkl} = \lambda\,\delta_{ij}\delta_{kl} + \mu(\delta_{ik}\delta_{jl} + \delta_{il}\delta_{jk})$, with λ, μ being the Lamé constants. $\mathbf{1}$ and $\mathbb{I}$ denoting the second-order and the fourth-order identity tensor, respectively. C is a material constant. The isotropic hardening function h is chosen as

$$h(p) = Q\,\{p - [1 - \exp(-bp)]/b\}\,, \tag{4}$$

where Q and b are material constants. The former stands for the asymptotic value of the isotropic hardening function. From the above three free energy functions we arrive at the corresponding stress-like counterparts

$$\boldsymbol{\sigma} = \frac{\partial \Psi}{\partial\, \boldsymbol{\varepsilon}^e} = \mathbb{C} : \boldsymbol{\varepsilon}^e, \qquad \boldsymbol{\alpha} = \frac{\partial \Psi}{\partial\, \boldsymbol{\xi}} = \frac{2}{3} C\,\boldsymbol{\xi}\,, \qquad R = \frac{\partial \Psi}{\partial p} = Q\,\{1 - \exp(-bp)\}\ . \tag{5}$$

In order to form the evolution equations of the internal variables $\boldsymbol{\varepsilon}^p$, p and $\boldsymbol{\xi}$, the concept of dissipation potential is applied and it is assumed that the normality rule is applicable[†], see Lemaitre and Chaboche [21], pp. 278–280. In this viscoplastic law the dissipation potential function Φ is assumed to consist of two decoupled parts: the plastic potential function ϕ_p and the recovery potential function ϕ_r, i.e.

$$\Phi = \phi_p(\boldsymbol{\sigma}, \boldsymbol{\alpha}, R) + \phi_r(\boldsymbol{\alpha}) \ , \tag{6}$$

with ϕ_p and ϕ_r defined by

$$\phi_p(\boldsymbol{\sigma}, \boldsymbol{\alpha}, R) = f(\boldsymbol{\sigma}, \boldsymbol{\alpha}, R) + \tfrac{1}{2a}\gamma(p) J_2^2(\boldsymbol{\alpha}) \ , \qquad \phi_r(\boldsymbol{\alpha}) = d\, J_2(\boldsymbol{\alpha})/C \ . \tag{7}$$

Where a, d and C are material constants. The plastic potential function ϕ_p consists of the yield function f and the second term, which is introduced to describe the effect of recall (or the fading memory effect) of kinematic hardening. The recovery potential function ϕ_r is applied to describe the restoration effect of plastic strain and the recovery effect of kinematic hardening. The function $J_2(\boldsymbol{\alpha})$ is defined by

$$J_2(\boldsymbol{\alpha}) = \sqrt{\tfrac{3}{2}\boldsymbol{\alpha} : \boldsymbol{\alpha}} \ . \tag{8}$$

$f(\boldsymbol{\sigma}, \boldsymbol{\alpha}, R)$ is the yield function

$$f(\boldsymbol{\sigma}, \boldsymbol{\alpha}, R) = J_2(\boldsymbol{s} - \boldsymbol{\alpha}) - k - R = \sqrt{\tfrac{3}{2}(\boldsymbol{s} - \boldsymbol{\alpha}) : (\boldsymbol{s} - \boldsymbol{\alpha})} - k - R \ , \tag{9}$$

with $\boldsymbol{s}$ being the deviator of the Cauchy stress tensor $\boldsymbol{\sigma}$, i.e. $\boldsymbol{s} = \boldsymbol{\sigma} - \frac{1}{3}(\mathrm{tr}\,\boldsymbol{\sigma})\mathbf{1}$. In equation (9) k stands for the initial yield strength. The function $\gamma(p)$ is defined as

$$\gamma(p) = \gamma_\infty + (1 - \gamma_\infty)\exp(-\omega p) \ , \tag{10}$$

where γ_∞ and ω are material constants. This function arises in the plastic potential function and can be used to adjust the center $\boldsymbol{\alpha}$ of the elastic domain.

[†]In some cases, for instance for anisotropic materials, the normality rule cannot furnish complete constitutive equations, as has been pointed out by Betten [9, 10] in more detail. Therefore, he developed modified flow rules for both incompressible and compressible anisotropic materials.

By extending the standard normality rule the evolution equations

$$\begin{aligned}
\dot{\boldsymbol{\varepsilon}}^p &= \dot{\lambda}_p \frac{\partial \phi_p}{\partial \boldsymbol{\sigma}} + \dot{\lambda}_s \frac{\partial \phi_r}{\partial \boldsymbol{\sigma}} = \dot{\lambda}_p \frac{\partial \phi_p}{\partial \boldsymbol{\sigma}} \,, \\
-\dot{\boldsymbol{\xi}} &= \dot{\lambda}_p \frac{\partial \phi_p}{\partial \boldsymbol{\alpha}} + \dot{\lambda}_s \frac{\partial \phi_r}{\partial \boldsymbol{\alpha}} \,, \\
-\dot{p} &= \dot{\lambda}_p \frac{\partial \phi_p}{\partial R} + \dot{\lambda}_s \frac{\partial \phi_r}{\partial R} = \dot{\lambda}_p \frac{\partial \phi_p}{\partial R} \,,
\end{aligned} \tag{11}$$

are obtained. In these formulations the independent plastic and static recovery multipliers $\dot{\lambda}_p$ and $\dot{\lambda}_s$ are applied. In the case of pure plasticity the plastic multiplier can be determined by the consistency condition $\dot{f}(\boldsymbol{\sigma}, \boldsymbol{\alpha}, R) = 0$. This condition means that in loading processes the stress always lies on the current yield surface. In the case of unified viscoplasticity the stress can lie outside the yield envelope. Therefore, the consistency condition is no more applicable. In this constitutive law the plastic multiplier is chosen as

$$\dot{\lambda}_p = \left[\frac{\langle f(\boldsymbol{\sigma}, \boldsymbol{\alpha}, R) \rangle}{K} \right]^m \,, \tag{12}$$

with K being the coefficient of resistance, m the hardening exponent. Where $\langle \cdot \rangle$ denotes the Macauley bracket with definition $\langle y \rangle = y$ if $y > 0$, and $\langle y \rangle = 0$ if $y \leq 0$. Alternatively, one can use the Heaviside unit function (see Betten [10]). The static recovery multiplier $\dot{\lambda}_s$ is also given as a power function

$$\dot{\lambda}_s = \left[\frac{J_2(\boldsymbol{\alpha})}{a} \right]^r \,, \tag{13}$$

where r is a material constant.

Application of equations (7)–(9) in equation (11) gives the evolution equations

$$\begin{aligned}
\dot{\boldsymbol{\varepsilon}}^p &= \frac{3}{2} \frac{\boldsymbol{s} - \boldsymbol{\alpha}}{J_2(\boldsymbol{s} - \boldsymbol{\alpha})} \dot{\lambda}_p \,, \\
\dot{\boldsymbol{\xi}} &= \dot{\boldsymbol{\varepsilon}}^p - \frac{3\gamma(p)\boldsymbol{\alpha}}{2a} \dot{\lambda}_p - \frac{3d}{2C} \frac{\boldsymbol{\alpha}}{J_2(\boldsymbol{\alpha})} \dot{\lambda}_s \\
\dot{p} &= \dot{\lambda}_p = \sqrt{\tfrac{2}{3} \dot{\boldsymbol{\varepsilon}}^p : \dot{\boldsymbol{\varepsilon}}^p} \,.
\end{aligned} \tag{14}$$

After getting the strain-like internal variables $\boldsymbol{\varepsilon}^p$, $\boldsymbol{\xi}$ and p by integrating these evolution equations we can compute the stress-like variables $\boldsymbol{\sigma}$, $\boldsymbol{\alpha}$ and R by virtue of equations (1) and (5). In fact,

one can directly formulate the evolution equations of the stress-like internal variables $\boldsymbol{\alpha}$ and R by combining $(5)_{2,3}$ with $(14)_{2,3}$; i.e.

$$\dot{\boldsymbol{\alpha}} = \tfrac{2}{3} C \dot{\boldsymbol{\varepsilon}}^p - \frac{C\gamma(p)\,\boldsymbol{\alpha}}{a}\dot{\lambda}_p - \frac{d\,\boldsymbol{\alpha}}{J_2(\boldsymbol{\alpha})}\dot{\lambda}_s\,, \qquad \dot{R} = b(Q-R)\dot{\lambda}_p\,. \tag{15}$$

Therefore, we can obtain the evolution functions $\boldsymbol{\alpha}$ and R directly by integrating the evolution equations in (15). Observing equation $(15)_1$ we note that the evolution equation of the back stress contains three mechanisms: the linear kinematic hardening and the effects of recall and recovery.

Obviously, this constitutive law can be applied only in processes with infinitesimal deformations. Some mathematical characteristics, e.g. the time derivatives $\dot{\boldsymbol{\varepsilon}}^p$, $\dot{\boldsymbol{\alpha}}$, confine the constitutive law to infinitesimal range. Since many metal structures, for example, metal plates and shells usually work in finite deformation states and finite deformations always arise in metal forming, it is necessary to extend the Chaboche law to finite deformation form, so that the advantages of this law can be exploited at finite deformations. In the next section an extension of this viscoplastic law will be presented based on an internal dissipation inequality.

3. The extended viscoplastic law at finite strains

For the extension of the Chaboche viscoplastic law we depart from the standard assumption for finite strain inelastic problems: the multiplicative decomposition of the deformation gradient $\boldsymbol{F}$ into an elastic and an inelastic part $\boldsymbol{F}^e$ and $\boldsymbol{F}^p$; i.e.

$$\boldsymbol{F} = \boldsymbol{F}^e \boldsymbol{F}^p. \tag{16}$$

About the micromechanical expositions of this decomposition and the consistency of the decomposition with plastic flow in metal plasticity we refer to Asaro [4, 5] and Asaro and Rice [6]. From the total deformation gradient we can express the left Cauchy-Green tensor $\boldsymbol{b}$ and the spatial logarithmic strain $\boldsymbol{h}$ as

$$\boldsymbol{b} = \boldsymbol{F}\boldsymbol{F}^{\mathrm{T}}, \qquad \boldsymbol{h} = \frac{1}{2}\ln \boldsymbol{b}. \tag{17}$$

In the theory of finite deformation the tensorial Hencky measure of strain and strain rate plays a central role (see Fitzgerald [19] and Betten [9]) because it can be decomposed into a sum of

an isochoric distorsion and a volume change. The problem to present the logarithmic function $\boldsymbol{Y} = \ln \boldsymbol{X}$ or $Y_{ij} = \{\ln \mathbf{X}\}_{ij}$ as an isotropic tensor function has been solved by Betten [7, 8]. In the same way, we can define the elastic left Cauchy-Green tensor $\boldsymbol{b}^e$ and the elastic logarithmic strain $\boldsymbol{h}^e$ from the elastic part of the deformation gradient; i.e.

$$\boldsymbol{b}^e = \boldsymbol{F}^e \boldsymbol{F}^{e\mathrm{T}}, \qquad \boldsymbol{h}^e = \frac{1}{2} \ln \boldsymbol{b}^e. \tag{18}$$

After knowing $\boldsymbol{b}^e$ we can determine the inelastic right Cauchy-Green tensor $\boldsymbol{C}^p$ by

$$\boldsymbol{C}^p = \boldsymbol{F}^{p\mathrm{T}} \boldsymbol{F}^p = \boldsymbol{F}^{\mathrm{T}} \boldsymbol{b}^{e-1} \boldsymbol{F}. \tag{19}$$

It has been proven by Lin [22] that for the finite strain inelastic problems with isotropic elasticity there is the internal dissipation inequality

$$\mathcal{D}_{\mathrm{int}} = \boldsymbol{\tau} : \left(\mathring{\boldsymbol{h}} - \mathring{\boldsymbol{h}}^e \right) \geq 0, \tag{20}$$

where $\mathcal{D}_{\mathrm{int}}$ is the energy dissipation per unit reference volume and unit time caused by inelastic deformation. $\boldsymbol{\tau}$ is the Kirchhoff stress, $\mathring{\boldsymbol{h}}$ and $\mathring{\boldsymbol{h}}^e$ denote the logarithmic corotational rates of the total logarithmic strain $\boldsymbol{h}$ and the elastic logarithmic strain $\boldsymbol{h}^e$, respectively. They are defined as

$$\mathring{\boldsymbol{h}} = \dot{\boldsymbol{h}} + \boldsymbol{h}\,\boldsymbol{\Omega} - \boldsymbol{\Omega}\,\boldsymbol{h}, \qquad \mathring{\boldsymbol{h}}^e = \dot{\boldsymbol{h}}^e + \boldsymbol{h}^e\,\boldsymbol{\Omega} - \boldsymbol{\Omega}\,\boldsymbol{h}^e, \tag{21}$$

with $\boldsymbol{\Omega}$ denoting the logarithmic spin. About a detailed account of the logarithmic spin the works of Xiao et al. [37, 38] can be consulted. In comparison with two extensively used dissipation inequalities: Simo's and Lion's inequalities (see e.g. Simo [32], Simo and Miehe [35] and Lion [28]), inequality (20) has a concise mathematical structure. This advantage can simplify the numerical implementation and the experimental identification of the constitutive laws based on this inequality. The inequality provides us also a dissipation-conjugate pair: the driving force $\boldsymbol{\tau}$ and the dissipation term $\mathring{\boldsymbol{h}} - \mathring{\boldsymbol{h}}^e$, which can be used to construct inelastic constitutive laws in the frame of thermodynamics.

Now, we return to the extension of the small strain Chaboche viscoplastic law. As well known, for finite strain inelastic problems the constitutive laws can be formulated in the current configuration, the reference configuration and in the (released) intermediate configuration. But, the constitutive

responses in the current configuration are usually required, therefore, we carry out the extension directly in the current configuration. For the extension we assume that the mathematical structures of the free energy and dissipation potential functions in equations (2) and (6) can be inherited at finite strains. We change the definitions of the arguments in these potential functions and reformulate the evolution equations of the internal variables so that the extended viscoplastic law satisfies the requirement of material frame indifference and is suitable for modeling finite strain viscoplastic problems. It should be noted that because of the requirement of material frame indifference all (independent and dependent) variables must be objective. According to the argument of Simo [33], pp. 331–332, the extended potential functions must be isotropic with respect to their arguments. According to the above assumptions the total free energy function Ψ has the formulation (2), with the elastic stored energy ψ_e redefined by Hencky's formulation; i.e.

$$\psi_e(\boldsymbol{h}^e) = \tfrac{1}{2}\boldsymbol{h}^e : \mathbb{C} : \boldsymbol{h}^e, \tag{22}$$

where $\mathbb{C}$ is the isotropic fourth-order elastic tensor defined after equation (3). For the free energies contributed by kinematic and isotropic hardenings we use here the same notations $\boldsymbol{\xi}$ and p for the arguments as in equations (2) and (4), but the definitions of the arguments are changed. Here, $\boldsymbol{\xi}$ is an objective and spatially described second-order tensor. Although p still denotes the accumulated plastic strain, it is defined here by the following formulation

$$p = \int_0^t \sqrt{\frac{2}{3}\left(\mathring{\boldsymbol{h}} - \mathring{\boldsymbol{h}}^e\right) : \left(\mathring{\boldsymbol{h}} - \mathring{\boldsymbol{h}}^e\right)}\, \mathrm{d}\tau. \tag{23}$$

The Kirchhoff stress $\boldsymbol{\tau}$ can be expressed as

$$\boldsymbol{\tau} = \frac{\partial \Psi}{\partial \boldsymbol{h}^e} = \mathbb{C} : \boldsymbol{h}^e. \tag{24}$$

For the computation of the stress-like internal variables $\boldsymbol{\alpha}$ and R the formulations $(5)_{2,3}$ are still applicable.

In the extended constitutive setting the mathematical structures of the dissipation potential functions, see equations (6)–(10), are also preserved. A small modification arises in the yield function f. Here, we use the Kirchhoff stress $\boldsymbol{\tau}$ to replace the original Cauchy stress tensor $\boldsymbol{\sigma}$.

Equation (9) is then reformulated as

$$f(\boldsymbol{\tau}, \boldsymbol{\alpha}, R) = J_2(\boldsymbol{s} - \boldsymbol{\alpha}) - k - R = \sqrt{\tfrac{3}{2}(\boldsymbol{s} - \boldsymbol{\alpha}) : (\boldsymbol{s} - \boldsymbol{\alpha})} - k - R, \tag{25}$$

with the deviatoric tensor $\boldsymbol{s}$ defined by $\boldsymbol{s} = \boldsymbol{\tau} - \frac{1}{3}(\mathrm{tr}\,\boldsymbol{\tau})\mathbf{1}$. It should be noted that by frame invariance the yield function f must be an isotropic function of its arguments. In fact, the difference $\boldsymbol{s} - \boldsymbol{\alpha}$ should be treated as an argument when the objectivity of the yield function f is considered. The reason is that any coordinate transformation transforms $\boldsymbol{s}$ and $\boldsymbol{\alpha}$ in the same way and does not change the mathematical form of the yield function. Therefore, the yield function fulfill the objective principle of materials.

By application of the dissipation-conjugate relation between $\boldsymbol{\tau}$ and $\mathring{\boldsymbol{h}} - \mathring{\boldsymbol{h}}^e$ at isotropic elasticity, we can trivially extend the evolution equation $(11)_1$ to the finite strain form

$$\mathring{\boldsymbol{h}}^{\log} - \mathring{\boldsymbol{h}}^e = \dot{\lambda}_p \frac{\partial \phi_p}{\partial\, \boldsymbol{\tau}} + \dot{\lambda}_s \frac{\partial \phi_r}{\partial\, \boldsymbol{\tau}} = \dot{\lambda}_p \frac{\partial \phi_p}{\partial\, \boldsymbol{\tau}}. \tag{26}$$

For the spatially described objective tensor $\boldsymbol{\xi}$ we postulate the evolution equation

$$-\mathring{\boldsymbol{\xi}} = \dot{\lambda}_p \frac{\partial \phi_p}{\partial \boldsymbol{\alpha}} + \dot{\lambda}_s \frac{\partial \phi_r}{\partial \boldsymbol{\alpha}}, \tag{27}$$

with $\mathring{\boldsymbol{\xi}}$ being the logarithmic corotational rate of $\boldsymbol{\xi}$, i.e. $\mathring{\boldsymbol{\xi}} = \dot{\boldsymbol{\xi}} + \boldsymbol{\xi}\,\boldsymbol{\Omega} - \boldsymbol{\Omega}\,\boldsymbol{\xi}$. The evolution equation of p is identical to equation $(11)_3$. In these evolution equations the multipliers $\dot{\lambda}_p$ and $\dot{\lambda}_s$ are assumed to keep their definitions at small strains, only with the involved yield function f defined by (25). With these new formulations in hand we can extend the formulations in (14) to the forms

$$\begin{aligned}
&\mathring{\boldsymbol{h}} - \mathring{\boldsymbol{h}}^e = \frac{3}{2}\frac{\boldsymbol{s} - \boldsymbol{\alpha}}{J_2(\boldsymbol{s} - \boldsymbol{\alpha})}\dot{\lambda}_p, \\
&\mathring{\boldsymbol{\xi}} = \frac{3}{2}\frac{\boldsymbol{s} - \boldsymbol{\alpha}}{J_2(\boldsymbol{s} - \boldsymbol{\alpha})}\dot{\lambda}_p - \frac{3\gamma(p)\boldsymbol{\alpha}}{2a}\dot{\lambda}_p - \frac{3d}{2C}\frac{\boldsymbol{\alpha}}{J_2(\boldsymbol{\alpha})}\dot{\lambda}_s, \\
&\dot{p} = \dot{\lambda}_p = \sqrt{\frac{2}{3}\left(\mathring{\boldsymbol{h}} - \mathring{\boldsymbol{h}}^e\right) : \left(\mathring{\boldsymbol{h}} - \mathring{\boldsymbol{h}}^e\right)}.
\end{aligned} \tag{28}$$

Taking the same procedure of formulating equation (15), we get the evolution equations for the stress-like internal variables $\boldsymbol{\alpha}$ and R at finite strains in contrast to (15); i.e.

$$\mathring{\boldsymbol{\alpha}} = \left[\frac{\boldsymbol{s} - \boldsymbol{\alpha}}{J_2(\boldsymbol{s} - \boldsymbol{\alpha})} - \frac{\gamma(p)\,\boldsymbol{\alpha}}{a}\right] C\dot{\lambda}_p - \frac{d\,\boldsymbol{\alpha}}{J_2(\boldsymbol{\alpha})}\dot{\lambda}_s, \qquad \dot{R} = b(Q - R)\dot{\lambda}_p. \tag{29}$$

For the convenience of the following numerical implementation the complete finite strain constitutive setting is summarized in Table 1.

Table 1: Finite viscoplastic law

Free energy functions:

$$\Psi = \psi_e(\boldsymbol{h}^e) + g(\boldsymbol{\xi}) + h(p) \ ,$$

$$\psi_e(\boldsymbol{h}^e) = \tfrac{1}{2}\boldsymbol{h}^e : \mathbb{C} : \boldsymbol{h}^e \ , \qquad g(\boldsymbol{\xi}) = \tfrac{1}{3} C\, \boldsymbol{\xi} : \boldsymbol{\xi} \ , \qquad h(p) = Q\,\{p - [1 - \exp(-bp)]/b\}$$

Kirchhoff stress and stress-like internal variables:

$$\boldsymbol{\tau} = \frac{\partial \Psi}{\partial \boldsymbol{h}^e} = \mathbb{C} : \boldsymbol{h}^e \ , \qquad \boldsymbol{\alpha} = \frac{\partial \Psi}{\partial\, \boldsymbol{\xi}} = \frac{2}{3} C\, \boldsymbol{\xi} \ , \qquad R = \frac{\partial \Psi}{\partial p} = Q\,\{1 - \exp(-bp)\}$$

Potential functions:

$$\Phi = \phi_p(\boldsymbol{\tau}, \boldsymbol{\alpha}, R) + \phi_r(\boldsymbol{\alpha}) \ ,$$

$$\phi_p(\boldsymbol{\tau}, \boldsymbol{\alpha}, R) = f(\boldsymbol{\tau}, \boldsymbol{\alpha}, R) + \tfrac{1}{2}\tfrac{1}{a}\gamma(p) J_2^2(\boldsymbol{\alpha}) \ , \qquad \phi_r(\boldsymbol{\alpha}) = d\, J_2(\boldsymbol{\alpha})/C \ ,$$

with

$$f(\boldsymbol{\tau}, \boldsymbol{\alpha}, R) = J_2(\boldsymbol{s} - \boldsymbol{\alpha}) - k - R = \sqrt{\tfrac{3}{2}(\boldsymbol{s} - \boldsymbol{\alpha}) : (\boldsymbol{s} - \boldsymbol{\alpha})} - k - R \ ,$$

$$\gamma(p) = \gamma_\infty + (1 - \gamma_\infty)\exp(-\omega p) \ , \qquad J_2(\boldsymbol{\alpha}) = \sqrt{\tfrac{3}{2}\,\boldsymbol{\alpha} : \boldsymbol{\alpha}} \ , \qquad \boldsymbol{s} = \boldsymbol{\tau} - \tfrac{1}{3}\operatorname{tr}\boldsymbol{\tau}\, \mathbf{1}$$

Evolution equations of strain-like internal variables:

$$\mathring{\boldsymbol{h}}^{\log} - \mathring{\boldsymbol{h}}^e = \dot{\lambda}_p \frac{\partial \phi_p}{\partial\, \boldsymbol{\tau}} = \frac{3}{2}\frac{\boldsymbol{s} - \boldsymbol{\alpha}}{J_2(\boldsymbol{s} - \boldsymbol{\alpha})}\dot{\lambda}_p \ ,$$

$$\mathring{\boldsymbol{\xi}} = -\dot{\lambda}_p \frac{\partial \phi_p}{\partial \boldsymbol{\alpha}} - \dot{\lambda}_s \frac{\partial \phi_r}{\partial \boldsymbol{\alpha}} = \frac{3}{2}\frac{\boldsymbol{s} - \boldsymbol{\alpha}}{J_2(\boldsymbol{s} - \boldsymbol{\alpha})}\dot{\lambda}_p - \frac{3\gamma(p)\boldsymbol{\alpha}}{2a}\dot{\lambda}_p - \frac{3d}{2C}\frac{\boldsymbol{\alpha}}{J_2(\boldsymbol{\alpha})}\dot{\lambda}_s \ ,$$

$$\dot{p} = -\dot{\lambda}_p \frac{\partial \phi_p}{\partial R} = \sqrt{\frac{2}{3}\left(\mathring{\boldsymbol{h}}^{\log} - \mathring{\boldsymbol{h}}^e\right) : \left(\mathring{\boldsymbol{h}}^{\log} - \mathring{\boldsymbol{h}}^e\right)} = \dot{\lambda}_p \ ,$$

with

$$\dot{\lambda}_p = \left[\frac{\langle f(\boldsymbol{\tau}, \boldsymbol{\alpha}, R)\rangle}{K}\right]^m \ , \qquad \dot{\lambda}_s = \left[\frac{J_2(\boldsymbol{\alpha})}{a}\right]^r$$

Evolution equations of stress-like internal variables:

$$\mathring{\boldsymbol{\alpha}} = \frac{\partial^2 \Psi}{\partial\, \boldsymbol{\xi}\, \partial\, \boldsymbol{\xi}}\mathring{\boldsymbol{\xi}} = \left[\frac{\boldsymbol{s} - \boldsymbol{\alpha}}{J_2(\boldsymbol{s} - \boldsymbol{\alpha})} - \frac{\gamma(p)\,\boldsymbol{\alpha}}{a}\right] C\dot{\lambda}_p - \frac{d\,\boldsymbol{\alpha}}{J_2(\boldsymbol{\alpha})}\dot{\lambda}_s \ ,$$

$$\dot{R} = \frac{\partial^2 \Psi}{\partial p \partial p}\dot{p} = b(Q - R)\dot{\lambda}_p$$

4. Algorithm aspects

In this section we present the numerical algorithm of determining the stress responses provided by the finite strain viscoplastic law. Since the constitutive law is nonlinear, the global Newton iterative procedure must be applied so that the stress field can be updated step by step. In this procedure the entire loading process must be divided into a sequence of loading steps. Correspondingly, the entire time interval $[0, T]$ is segmented into $[0, T] = \bigcup_{n=0}^{m} \mathbb{I}_n$, with $\mathbb{I}_n = [t_n, t_{n+1}]$ denoting a time interval. We assume that the constitutive state at instant t_n is given. This means that we know the deformation gradient $\boldsymbol{F}_n$, the stress $\boldsymbol{\tau}_n$, as well as all internal variables $\boldsymbol{h}^e_n$, $\boldsymbol{\xi}_n$, p_n, $\boldsymbol{\alpha}_n$ and R_n at this instant. Further, it is assumed that the deformation gradient $\boldsymbol{F}_{n+1}$ at instant t_{n+1} is known, the goal of the numerical algorithm is to determine the internal variables $\boldsymbol{h}^e_{n+1}$, $\boldsymbol{\xi}_{n+1}$, p_{n+1}, $\boldsymbol{\alpha}_{n+1}$, R_{n+1} and the stress $\boldsymbol{\tau}_{n+1}$ at time t_{n+1}.

Let $\Delta\boldsymbol{Q}$ be the rotation increment of the logarithmic corotational coordinate frame rotated by the logarithmic spin $\boldsymbol{\Omega}$ over time increment $\Delta t = t_{n+1} - t_n$. Then, the elastic logarithmic strain $\boldsymbol{h}^e_{n+1}$ and the internal variable $\boldsymbol{\alpha}_{n+1}$ at instant t_{n+1} can be expressed by virtue of a backward Euler scheme as

$$\boldsymbol{h}^e_{n+1} = \Delta\boldsymbol{Q}\boldsymbol{h}^e_n\Delta\boldsymbol{Q}^{\mathrm{T}} + \mathring{\boldsymbol{h}}^e_{n+1}\Delta t, \qquad \boldsymbol{\alpha}_{n+1} = \Delta\boldsymbol{Q}\boldsymbol{\alpha}_n\Delta\boldsymbol{Q}^{\mathrm{T}} + \mathring{\boldsymbol{\alpha}}_{n+1}\Delta t. \tag{30}$$

Now, we define a trial elastic logarithmic strain

$$\boldsymbol{h}^{e\,\mathrm{tr}}_{n+1} = \Delta\boldsymbol{Q}\boldsymbol{h}^e_n\Delta\boldsymbol{Q}^{\mathrm{T}} + \mathring{\boldsymbol{h}}_{n+1}\Delta t. \tag{31}$$

With these tensors in hand application of the backward Euler scheme to equation $(28)_{1,3}$ and (29) yields the local discrete evolution equations

$$\begin{aligned}
\boldsymbol{h}^e_{n+1} &= \boldsymbol{h}^{e\,\mathrm{tr}}_{n+1} - \frac{3}{2}\frac{\boldsymbol{s}_{n+1} - \boldsymbol{\alpha}_{n+1}}{J_2(\boldsymbol{s}_{n+1} - \boldsymbol{\alpha}_{n+1})}\Delta\lambda_{p\,n+1},\\
\boldsymbol{\alpha}_{n+1} &= \boldsymbol{\alpha}'_n + \left[\frac{\boldsymbol{s}_{n+1} - \boldsymbol{\alpha}_{n+1}}{J_2(\boldsymbol{s}_{n+1} - \boldsymbol{\alpha}_{n+1})} - \frac{\gamma(p_{n+1})\,\boldsymbol{\alpha}_{n+1}}{a}\right] C\Delta\lambda_{p\,n+1} - \frac{d\,\boldsymbol{\alpha}_{n+1}}{J_2(\boldsymbol{\alpha}_{n+1})}\Delta\lambda_{s\,n+1},\\
R_{n+1} &= R_n + b(Q - R_{n+1})\Delta\lambda_{p\,n+1},\\
p_{n+1} &= p_n + \Delta\lambda_{p\,n+1}.
\end{aligned} \tag{32}$$

Here, $\boldsymbol{\alpha}'_n = \Delta\boldsymbol{Q}\boldsymbol{\alpha}_n\Delta\boldsymbol{Q}^{\mathrm{T}}$, $\Delta\lambda_{p\,n+1} = \dot{\lambda}_{p\,n+1}\Delta t$ and $\Delta\lambda_{s\,n+1} = \dot{\lambda}_{s\,n+1}\Delta t$. This algorithm is similar to the return mapping algorithm for the rate-independent plasticity, although here the stress can stay outside the yield surface. Obviously, these evolution equations are implicit. For solving them a Newton iterative procedure is usually needed. In equation (32) the discrete evolution equation for $\boldsymbol{\xi}_{n+1}$ is not applied, as in the constitutive setting all evolution equations are not directly dependent on the strain-like internal variable $\boldsymbol{\xi}$. Obviously, the above formulated discrete evolution equations depend on the rotation tensor $\Delta\boldsymbol{Q}$. For the computation of this rotation tensor, one can apply the logarithmic spin tensor (see Xiao et al. [37, 38]) specifying the rotation of the logarithmic corotational coordinate frame and make use of an exponential mapping procedure (see e.g. Simo and Hughes [34], pp. 297).

Introduce the notation $\boldsymbol{\tau}^{\mathrm{tr}}$ to denote the trial Kirchhoff stress and $\boldsymbol{s}^{\mathrm{tr}}$ to denote its deviator. Then, we have

$$\boldsymbol{\tau}^{\mathrm{tr}} = \mathbb{C} : \boldsymbol{h}^{e\,\mathrm{tr}}, \qquad \boldsymbol{s}^{\mathrm{tr}} = 2\mu\bar{\boldsymbol{h}}^{e\,\mathrm{tr}}, \qquad \boldsymbol{s} = 2\mu\bar{\boldsymbol{h}}^{e}, \tag{33}$$

with $\bar{\boldsymbol{h}}^{e}$ and $\bar{\boldsymbol{h}}^{e\,\mathrm{tr}}$ being the deviatoric parts of $\boldsymbol{h}^{e}$ and $\boldsymbol{h}^{e\,\mathrm{tr}}$; i.e. $\bar{\boldsymbol{h}}^{e} = \boldsymbol{h}^{e} - \frac{1}{3}(\mathrm{tr}\,\boldsymbol{h}^{e})\mathbf{1}$ and $\bar{\boldsymbol{h}}^{e\,\mathrm{tr}} = \boldsymbol{h}^{e\,\mathrm{tr}} - \frac{1}{3}(\mathrm{tr}\,\boldsymbol{h}^{e\,\mathrm{tr}})\mathbf{1}$. Further, let $\boldsymbol{\nu} = (\boldsymbol{s} - \boldsymbol{\alpha})/\|\boldsymbol{s} - \boldsymbol{\alpha}\|$. Then, application of equations (24), $(33)_1$ and the definition of $\boldsymbol{\nu}$ to $(32)_1$ yields $\boldsymbol{\tau}_{n+1} = \boldsymbol{\tau}^{\mathrm{tr}}_{n+1} - \sqrt{\frac{3}{2}}\Delta\lambda_{p\,n+1}\mathbb{C} : \boldsymbol{\nu}_{n+1}$. Due to $\boldsymbol{\nu} : \mathbf{1} = 0$ we have

$$\mathrm{tr}\,\boldsymbol{\tau} = \mathrm{tr}\,\boldsymbol{\tau}^{\mathrm{tr}}, \qquad \boldsymbol{s}_{n+1} = \boldsymbol{s}^{\mathrm{tr}}_{n+1} - \sqrt{6}\mu\Delta\lambda_{p\,n+1}\,\boldsymbol{\nu}_{n+1}\,. \tag{34}$$

From $(32)_2$ one can derive

$$\boldsymbol{\alpha}_{n+1} = \left[\boldsymbol{\alpha}'_n + \sqrt{\tfrac{2}{3}}\,C\Delta\lambda_{p\,n+1}\,\boldsymbol{\nu}_{n+1}\right]/M_{n+1}, \tag{35}$$

where $M_{n+1} = 1 + C\Delta\lambda_{p\,n+1}\gamma(p_{n+1})/a + d\Delta\lambda_{s\,n+1}/J_2(\boldsymbol{\alpha}_{n+1})$. It should be noted here that M_{n+1} can be treated as a function of the independent back stress $\boldsymbol{\alpha}_{n+1}$ and plastic multiplier $\Delta\lambda_{p\,n+1}$, since the other two variables: the accumulated plastic strain p_{n+1} and the static recovery multiplier $\Delta\lambda_{s\,n+1}$ depend explicitly on $\Delta\lambda_{p\,n+1}$ and $\boldsymbol{\alpha}_{n+1}$, respectively. See (13) and $(32)_4$. Subtraction of (35) from $(34)_2$ implies

$$\boldsymbol{s}_{n+1} - \boldsymbol{\alpha}_{n+1} = (\boldsymbol{s}^{\mathrm{tr}}_{n+1} - \boldsymbol{\alpha}'_n/M_{n+1}) - \sqrt{\tfrac{2}{3}}(3\mu + C/M_{n+1})\Delta\lambda_{p\,n+1}\,\boldsymbol{\nu}_{n+1}\,. \tag{36}$$

According to the definition of $\boldsymbol{\nu}$ we know that $\boldsymbol{s}_{n+1} - \boldsymbol{\alpha}_{n+1}$ is coaxial to $\boldsymbol{\nu}_{n+1}$. Therefore, we have

$$\boldsymbol{\nu}_{n+1} = (\boldsymbol{s}^{\mathrm{tr}}_{n+1} - \boldsymbol{\alpha}'_n/M_{n+1})/\|\boldsymbol{s}^{\mathrm{tr}}_{n+1} - \boldsymbol{\alpha}'_n/M_{n+1}\|. \tag{37}$$

It can be easily seen from this equation that $\boldsymbol{\nu}_{n+1}$ is dependent on $\Delta\lambda_{p\,n+1}$ and $\boldsymbol{\alpha}_{n+1}$, but independent of the stress tensor $\boldsymbol{\tau}_{n+1}$. Therefore, equation (35) also depends on the two variables $\Delta\lambda_{p\,n+1}$ and $\boldsymbol{\alpha}_{n+1}$ only. By making use of (12) (with the yield function f defined by (25)) and (36) we can derive another implicit equation for the plastic loading situations

$$\Delta\lambda_{p\,n+1} = \Delta t \left[\frac{\langle J_2(\boldsymbol{s}^{\mathrm{tr}}_{n+1} - \boldsymbol{\alpha}'_n/M_{n+1}) - (3\mu + C/M_{n+1})\Delta\lambda_{p\,n+1} - k - R_{n+1}\rangle}{K} \right]^m. \tag{38}$$

Obviously, this equation also includes two variables $\Delta\lambda_{p\,n+1}$ and $\boldsymbol{\alpha}_{n+1}$ only. Therefore, equations (35) and (38) consist of an implicit equation set, which can be used to solve the back stress $\boldsymbol{\alpha}_{n+1}$ and the plastic multiplier $\Delta\lambda_{p\,n+1}$. After getting the two variables the other quantities at time t_{n+1} can be trivially determined by the corresponding explicit equations.

Remark. If the static recovery effect is omitted (i.e. $\dot{\lambda}_s \equiv 0$) M_{n+1}, and therefore, $\boldsymbol{\nu}_{n+1}$ and $\boldsymbol{\alpha}_{n+1}$ can be expressed as the explicit functions of the plastic multiplier $\Delta\lambda_{p\,n+1}$. In this situation equation (38) is independent of the back stress $\boldsymbol{\alpha}_{n+1}$. The only needed local iterative procedure is for solving $\Delta\lambda_{p\,n+1}$ from equation (38). Further, if the relaxation effect is also negligible (i.e. $\gamma(p) \equiv 0$) the constitutive model reduces to the classical unified viscoplastic model of J_2-flow theory. In this case $M_{n+1} = 1$, and $\boldsymbol{\nu}_{n+1} = (\boldsymbol{s}^{\mathrm{tr}}_{n+1} - \boldsymbol{\alpha}'_n)/\|\boldsymbol{s}^{\mathrm{tr}}_{n+1} - \boldsymbol{\alpha}'_n\|$ is constant in the return mapping process.

In finite element implementation of a mechanical field problem the central field equation necessarily to be solved is the spatial discrete equation derived from the weak form of the balance equation of linear momentum. By linearization of the weak form of the balance equation one can obtain the definition of the exact consistent or algorithmic tangent modulus. With spatial description and omitting the subscript $n+1$ the definition of the consistent tangent modulus is included in the rate equation $\pounds_{\boldsymbol{v}}\boldsymbol{\tau} = \mathbb{C}^{ep} : \boldsymbol{d}$ (see Simo [33], pp. 365–368). Here, $\mathbb{C}^{ep}$ is the fourth-order consistent tangent modulus, while $\pounds_{\boldsymbol{v}}\boldsymbol{\tau}$ and $\boldsymbol{d}$ denote the Lie-derivative of the Kirchhoff stress $\boldsymbol{\tau}$ with respect to the "flow" specified by the total deformation and the deformation rate tensor, respectively. Here,

we use however the following formulation to define the algorithmic tangent modulus; i.e.

$$\mathbb{C}^{ep} = \boldsymbol{Q}^{*}(\bar{\mathbb{C}}^{ep}), \qquad \text{with} \quad \bar{\mathbb{C}}^{ep} = \partial \boldsymbol{T} / \partial \boldsymbol{H}. \tag{39}$$

Where $\boldsymbol{T}$ and $\boldsymbol{H}$ are, respectively, the counterparts of the Kirchhoff stress $\boldsymbol{\tau}$ and the logarithmic strain $\boldsymbol{h}$ in the logarithmic corotational coordinate system, i.e. $\boldsymbol{T} = \boldsymbol{Q}^{\mathrm{T}}\,\boldsymbol{\tau}\,\boldsymbol{Q}$ and $\boldsymbol{H} = \boldsymbol{Q}^{\mathrm{T}}\boldsymbol{h}\,\boldsymbol{Q}$, with $\boldsymbol{Q}$ being the logarithmic rotation tensor. $\boldsymbol{Q}^{*}(\bar{\mathbb{C}}^{ep})$ denotes the push-forward of the fourth-order tensor $\bar{\mathbb{C}}^{ep}$ by the rotation tensor $\boldsymbol{Q}$. From (39), it can be easily seen that the key point to compute the algorithmic tangent modulus $\mathbb{C}^{ep}$ is the calculation of the tangent modulus $\bar{\mathbb{C}}^{ep}$. According to Eq. (31) we know that the current increment of $\boldsymbol{H}$ is identical to the increment used in the trial elastic strain $\boldsymbol{H}^{e\,\mathrm{tr}} = \boldsymbol{Q}^{\mathrm{T}}\boldsymbol{h}^{e\,\mathrm{tr}}\,\boldsymbol{Q}$, therefore we have $\partial \boldsymbol{T} / \partial \boldsymbol{H} = \partial \boldsymbol{T} / \partial \boldsymbol{H}^{e\,\mathrm{tr}}$.

It should be noted that the formulation of the algorithmic modulus $\bar{\mathbb{C}}^{ep}$ is an arduous task, since the rotated Kirchhoff stress $\boldsymbol{T}$ are not directly dependent on the trial elastic strain $\boldsymbol{H}^{e\,\mathrm{tr}}$. For this formulation the stress-strain relation (24) and almost all evolution equations must be applied. By application of the chain rule, the stress-strain relation (24) and the evolution equations included in (32) and after a lengthy calculation we get

$$\bar{\mathbb{C}}^{ep} = \frac{\partial \boldsymbol{T}}{\partial \boldsymbol{H}^{e\,\mathrm{tr}}} = \frac{\partial \boldsymbol{T}}{\partial \boldsymbol{H}^{e}} : \frac{\partial \boldsymbol{H}^{e}}{\partial \boldsymbol{H}^{e\,\mathrm{tr}}} = \mathbb{C} : \mathbb{K}^{-1}\,, \tag{40}$$

with $\mathbb{C}$ being the elastic modulus defined after (3), $\mathbb{K}$ denoting a fourth-order tensor. About the detailed formulation of $\mathbb{K}$ see Appendix.

5. Numerical examples

In oder to prove the effectivity and reliability of the finite viscoplastic law and the numerical algorithm several numerical examples are presented in this section. In the first example the numerical simulations of uniaxial tension under five different deforming rates are compared with experimental observations. The second example presents a numerical prediction of the viscoplastic law under cyclic uniaxial loading, the numerical simulation is further compared with an experimental observation in the last loading cycle. In the third and fourth examples two forming processes with large deformations and rotations as well as complex contact boundary conditions are simulated. For

these examples we use the material parameters for the Ni-base supper alloy IN738 LC at 850°C, which are shown in Table 2.

Table 2: Material parameters for IN738 LC at 850°C [30, 31]

$E = 149650$ MPa	$\nu = 0.33$	$k = 153$ MPa	$C = 62511$ MPa
$b = 317$	$Q = -153$ MPa	$K = 1150$ MPa·s$^{1/m}$	$m = 7.7$
$a = 311$ MPa	$r = 4.8$	$d = 0.0227$ MPa·s^{-1}	$\gamma_\infty = 1.1$
$\omega = 0.04$			

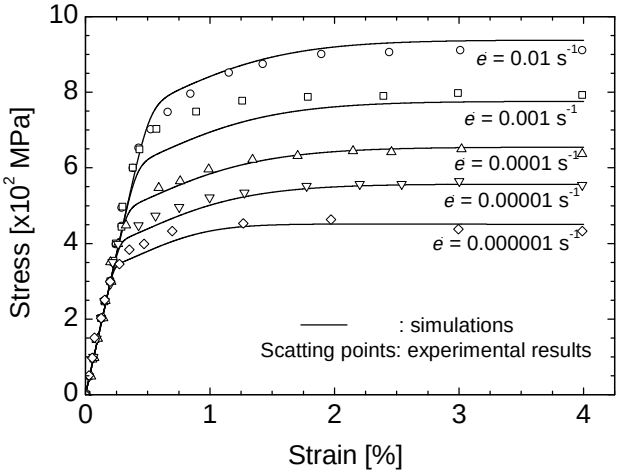

Fig. 2: Stress-strain response of IN738 LC at 850°C and uniaxial tension

5.1. Stress-strain response at uniaxial tension

In this example five uniaxial tensile tests of IN738 LC at temperature 850°C and strain rates $\dot{\varepsilon} = 0.01$, 0.001, 0.0001, 0.00001 and 0.000001 s^{-1} are simulated. The numerical predictions and experimental observations are illustrated in Fig. 2. Obviously, the numerical predictions agree well with the experimental data. Only in the neighborhood of the yield point on the curve corresponding to strain rate 0.001 s^{-1} we find a clear difference between both results. For the five strain rate cases there are clear elastic regimes on the stress-strain curves. At the beginning phases of plastic flow, strain-hardening enlarges the yield strength. With increasing strain the strain-hardening effect fades away and the softening effect appears more and more clearly.

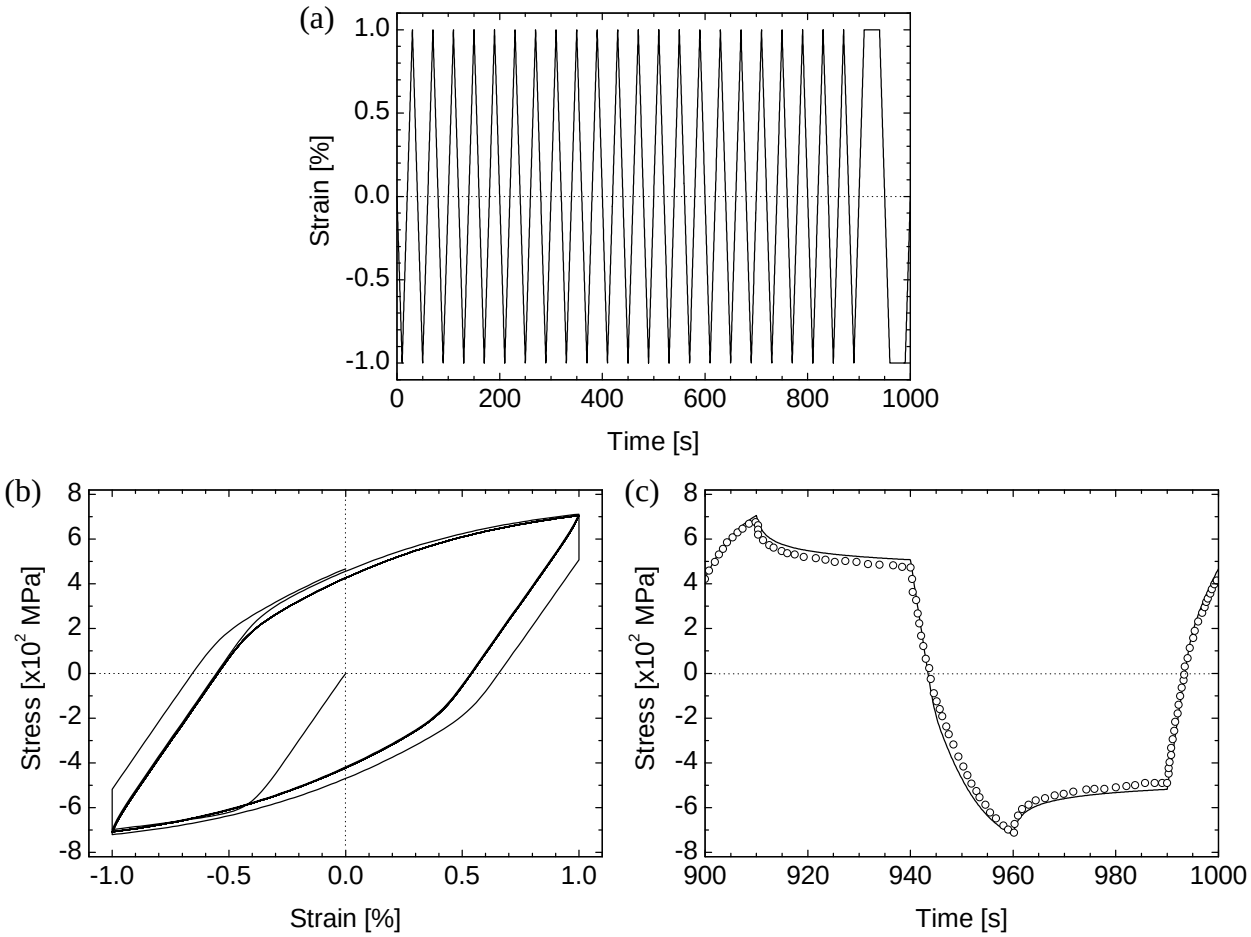

Fig. 3: Stress response of IN738 LC under cyclic uniaxial loading. (a) strain history, (b) numerical stress-strain response and (c) comparison between model prediction and experimental observation in the last loading cycle

5.2. Stress response at cyclic uniaxial loading

In this example a comparison of a prediction of the viscoplastic law with experimental results at cyclic uniaxial loading is carried out. Limited by the existing experimental data this comparison is accomplished only at small strains. Fig. 3(a) shows the history of the strain component in the loading direction. Under total 23 cycles the first 22 cycles have an identical strain trace. In the last strain cycle the strain keeps constant at maximum and minimum respectively in the time intervals [910, 940] s and [960, 990] s. Fig. 3(b) shows the numerical simulation of the stress-strain response in the entire cyclic loading process. It can be seen that except the first and last ones the other strain-stress cycles are almost identical. This means that there is no obvious isotropic hardening in these cycles. In contrast, kinematic hardening and the Bausinger effect can be easily seen. Due to stress

relaxation the last strain-stress cycle is different from the other cycles clearly. Fig. 3(c) illustrates the experimental observation and the numerical simulation in the last strain cycle. The experimental data are obtained from a cyclic uniaxial test on a cylinder made of the Ni-based super alloy IN 738 LC at 850°C [31]. From Fig. 3(c) we can see that after 22 strain cycles the numerical prediction agrees still well with the experimental observation. This proves that the viscoplastic law is effective even at complex cyclic loading.

5.3. Mechanical response in billet upsetting

In this example we presents the simulation of the upsetting of an axisymmetric billet. The material of the billet is assumed also to be the Ni-based super alloy IN738 LC at 850°C and the material parameters in Table 2 are applied to this simulation. The initial radius and height of the billet

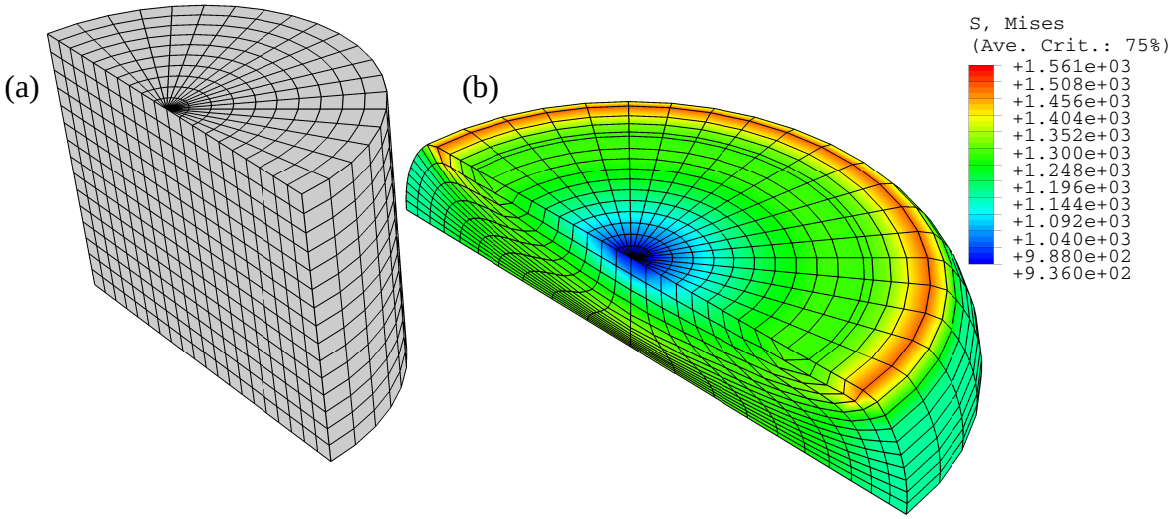

Fig. 4: Billet upsetting. (a) initial meshes and (b) von Mises stress contour at 10 s

are 10 and 30 mm, respectively. In ten seconds the billet is upset to 38% original height. Then, this upsetting is kept for five seconds. Because the symmetry of the problem only one-eighth of the billet is used for the simulation and 10×15 quadrilateral axisymmetric solid elements are applied. Fig. 4(a) is obtained by an 180-degree-sweep of the initial elements and shows one-fourth of the billet. The corresponding deformed meshes and the contours of von Mises stress at time 10 s are illustrated in Fig. 4(b). According to the deformed meshes we know that large deformations and rotations occur in an outside cyclic zone beneath the upper contact surface. The maximum

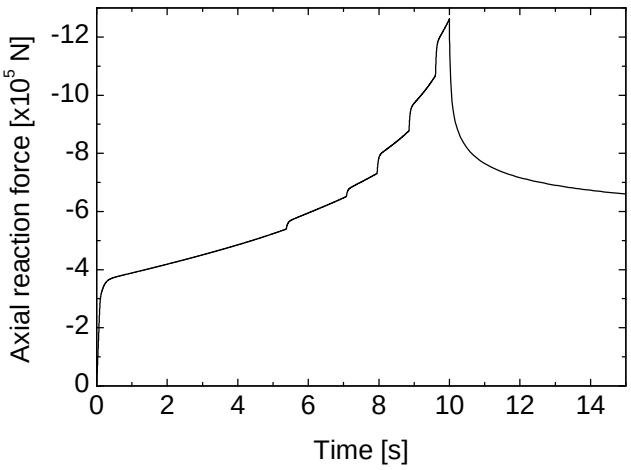

Fig. 5: Billet upsetting. Axial reaction force history

von Mises stress appears also in this zone. The minimum stress lies at the center of the upper surface. Fig. 4(c) illustrates the history of the axial reaction force. At the beginning the reaction force increases rapidly. In this phase the global deformation is elastic. Then, the billet goes into a global plastic state and the reaction force increases slowly. After 5 s there are five skip points on the curve. These skips are caused by the change of contact nodes. In the phase of relaxation the curve is smooth and about one-half of the reaction force at time 10 s is relaxed.

5.4. Mechanical response in channel forming

This example presents the mechanical responses in the forming process of a channel. Figure 6(a) illustrates the dimensions of the components and the forming process schematically. The dimensions and geometries of the components are selected according to an example in [1]. Because of the symmetry of the problem only the right half of the components is taken and applied to the simulation. The right part of the blank is hold by the die and the blank holder. The another part is pressed downwards by the punch up to a maximum punch displacement of 0.03 m. The punch, die and blank holder are assumed to be rigid and the blank be always in plane strain state, i.e. the normal strain component in the third direction is always zero. The Coulomb friction is assumed to exist between the blank and the rigid bodies with the friction coefficient being 0.1. In the first four seconds the contact conditions between the blank and die as well as the holder are established and the holder force of 440000 N is applied by the blank holder. In time interval [4, 5] s the punch moves

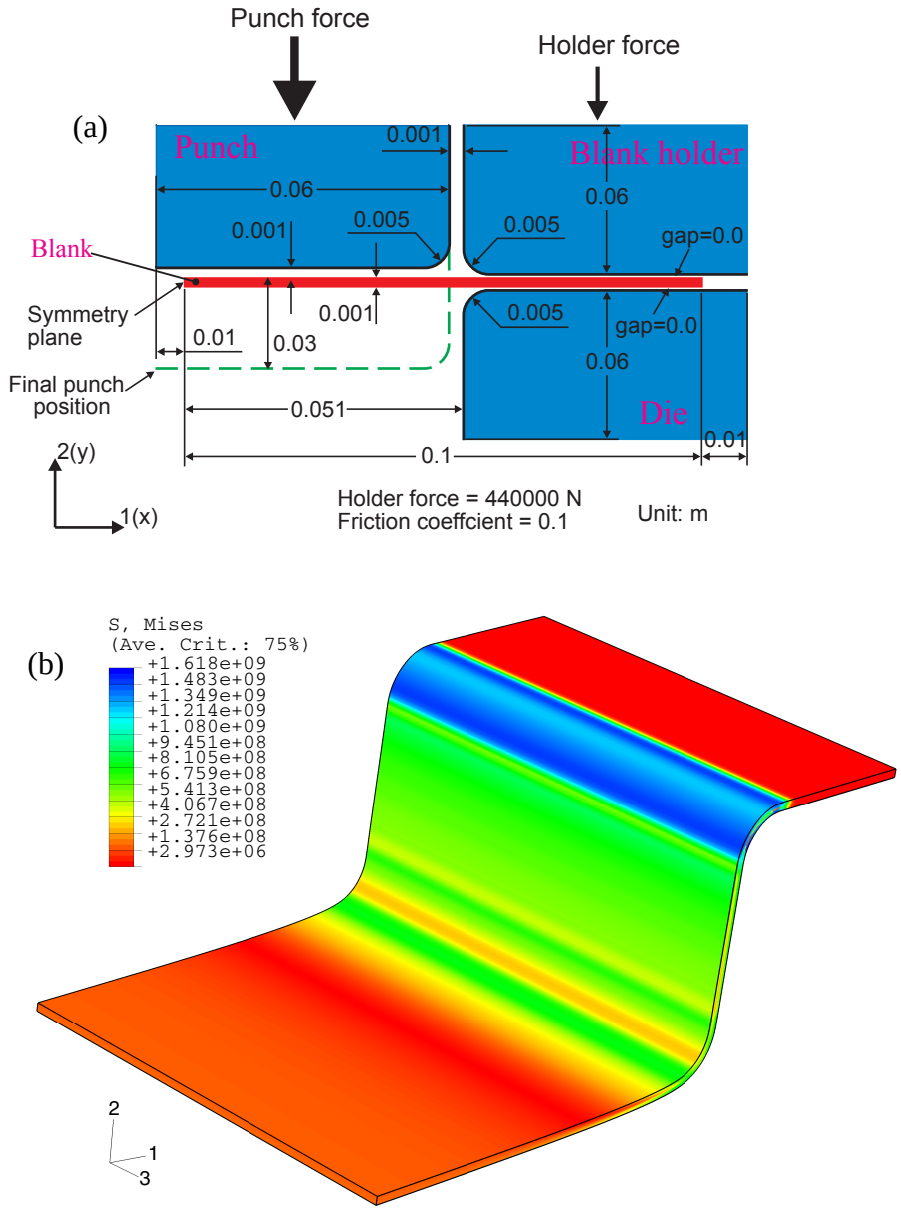

Fig. 6: Forming a channel. (a) schematic diagram of the components and dimensions, (b) von Mises stress contour at time 5 s

down uniformly and the channel is formed. Here, the forming process is assumed to be quasi-static. Therefore, the dynamic effect is neglected. Fig. 6(b) shows the deformed blank configuration and the distribution of the von Mises stress at time 5 s. The maximum stress appears in the zone on the upper corner of the deformed blank. The blank thickness in this zone reduces clearly. The stresses distributed in the part parallel to the coordinate direction 2 are larger than those in the two parts rectangular to the direction. The plastic flow occurs mainly in the zone from the upper corner to the lower corner, therefore the blank in this zone is thinner than that in other zones. In Fig. 7 the history of the reaction force R_2 in the direction 2 is illustrated. In the first four seconds the punch

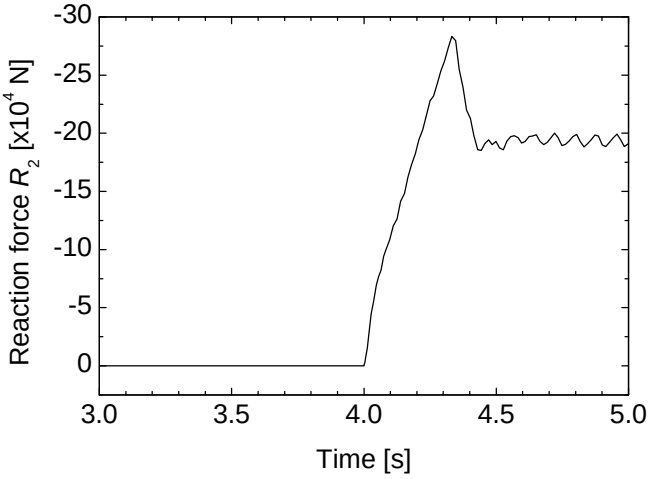

Fig. 7: Forming a channel. Reaction force history in direction 2

does not press on the blank the reaction force R_2 vanishes therefore in this interval. In the interval [4, 5] s, R_2 increases first very quickly and reaches its maximum at time 4.33 s. Then, the reaction force turns back to values where it oscillates with the increasing time.

6. Conclusions

This work presents a finite viscoplastic law extended from an infinitesimal Chaboche viscoplastic law. By virtue of an internal dissipation inequality, with the Kirchhoff stress being the driving force and the difference of the logarithmic corotational rates of the total and the elastic logarithmic strains being the dissipation term, the viscoplastic law is formulated in the spatial configuration. The evolution equation of the strain-like internal variable conjugate to the spatial back stress is also described in terms of its logarithmic corotational rate. The finite viscoplastic law is consistent with the second law of thermodynamics. An implicit integration procedure is established. The numerical algorithms for integrating the internal variables and the consistent tangent moduli are formulated. Several numerical examples are presents and the numerical predictions are compared with the experimental observations under monotonic and cyclic uniaxial loading. These comparisons show a good consistency between the theoretical predictions and the experimental observations. Other two numerical examples with large deformations and rotations as well as complex contact boundary conditions prove the effectivity and reliability of the algorithms.

Appendix

In this appendix the detailed algorithmic modulus tensor $\mathbb{K}$ is formulated. For clarity the subscripts $n+1$ of all corresponding quantities are omitted. Here, we record, according to (32), a set of discrete evolution equations described in the logarithmic corotational coordinate system

$$\begin{aligned}
\boldsymbol{H}^{e\,\mathrm{tr}} &= \boldsymbol{H}^{e} + \frac{3}{2}\frac{\boldsymbol{S}-\boldsymbol{\beta}}{J_2(\boldsymbol{S}-\boldsymbol{\beta})}\Delta\lambda_p,\\
\boldsymbol{\beta} &= \boldsymbol{\beta}_n + \left[\frac{\boldsymbol{S}-\boldsymbol{\beta}}{J_2(\boldsymbol{S}-\boldsymbol{\beta})} - \frac{\gamma(p)\boldsymbol{\beta}}{a}\right] C\Delta\lambda_p - \frac{d\boldsymbol{\beta}}{J_2(\boldsymbol{\beta})}\Delta\lambda_s,\\
R &= R_n + b(Q-R)\Delta\lambda_p,\\
p &= p_n + \Delta\lambda_p,
\end{aligned} \tag{A1}$$

with

$$\Delta\lambda_p = \left[\frac{\langle J_2(\bar{\boldsymbol{\beta}}-\boldsymbol{\theta}) - k - R\rangle}{K}\right]^m \Delta t, \qquad \Delta\lambda_s = \left[\frac{J_2(\boldsymbol{\theta})}{a}\right]^r \Delta t. \tag{A2}$$

Where $\boldsymbol{H}^e$, $\boldsymbol{H}^{e\,\mathrm{tr}}$, $\boldsymbol{S}$, $\boldsymbol{\beta}$ and $\boldsymbol{\beta}_n$ are the pull-backs of the spatial tensors $\boldsymbol{h}^e$, $\boldsymbol{h}^{e\,\mathrm{tr}}$, $\boldsymbol{s}$, $\boldsymbol{\alpha}$ and $\boldsymbol{\alpha}'_n$; i.e. $\boldsymbol{X} = \boldsymbol{Q}^{\mathrm{T}}\boldsymbol{Y}\boldsymbol{Q}$, with $\boldsymbol{X}$ and $\boldsymbol{Y}$ being the corresponding tensors in the former and latter sets above and $\boldsymbol{Q}$ denoting the logarithmic rotation tensor. From $(\mathrm{A1})_{3,4}$ we can easily derive

$$\frac{\partial p}{\partial\,\boldsymbol{\eta}^e} = \frac{\partial\Delta\lambda_p}{\partial\,\boldsymbol{\eta}^e}, \qquad \frac{\partial R}{\partial\,\boldsymbol{\eta}^e} = A_1\frac{\partial\Delta\lambda_p}{\partial\,\boldsymbol{\eta}^e}, \tag{A3}$$

with $A_1 = \frac{b(Q-R_n)}{(1+b\Delta\lambda_p)^2}$. By using the relation $\boldsymbol{S} = 2\mu\mathbb{P} : \boldsymbol{H}^e$, with $\mathbb{P} = \mathbb{I} - \frac{1}{3}\mathbf{1}\otimes\mathbf{1}$[‡], and the chain rule we arrive at

$$\frac{\partial\boldsymbol{S}}{\partial\boldsymbol{H}^e} = 2\mu\mathbb{P}, \qquad \frac{\partial J_2(\boldsymbol{S}-\boldsymbol{\beta})}{\partial\boldsymbol{H}^e} = \sqrt{\tfrac{3}{2}}\,\boldsymbol{\nu} : \left[2\mu\mathbb{P} - \frac{\partial\boldsymbol{\beta}}{\partial\boldsymbol{H}^e}\right], \tag{A4}$$

where $\boldsymbol{\nu} = (\boldsymbol{S}-\boldsymbol{\beta})/\|\boldsymbol{S}-\boldsymbol{\beta}\|$. With the relations $(\mathrm{A3})_2$ and $(\mathrm{A4})_2$ in hand one gets from $(\mathrm{A2})_1$

$$\frac{\partial\Delta\lambda_p}{\partial\boldsymbol{H}^e} = \sqrt{\tfrac{3}{2}}A_3\,\boldsymbol{\nu} : \left[2\mu\mathbb{P} - \frac{\partial\boldsymbol{\beta}}{\partial\boldsymbol{H}^e}\right], \tag{A5}$$

[‡]The fourth-order tensor $\mathbb{P}$ can be expressed in index-notation [9, 10] as $\mathbb{P}_{ijkl} = \frac{1}{2}(\delta_{ik}\delta_{jl} + \delta_{il}\delta_{jk}) - \frac{1}{3}\delta_{ij}\delta_{kl}$. This tensor is deviatoric with respect to both the first and second index pairs, i.e.: $\mathbb{P}_{jjkl} = \mathbf{0}_{kl}$ and $\mathbb{P}_{ijkk} = \mathbf{0}_{ij}$, where $\mathbf{0}_{ij}$ is the second-order zero tensor. Thus, one can interpret $\mathbb{P}$ as a deviatoric part of the fourth-order identity tensor $\mathbb{I}$.

where $A_3 = \frac{A_2}{1+A_1A_2}$, with $A_2 = \frac{m\Delta t}{K}\left[\frac{\langle J_2(\tilde{\boldsymbol{\beta}}-\boldsymbol{\theta})-k-R\rangle}{K}\right]^{m-1}$. Recalling $\gamma(p) = \gamma_\infty + (1-\gamma_\infty)\exp(-\omega p)$, and exploiting equations $(A3)_1$, (A5) we obtain

$$\frac{\partial \gamma(p)}{\partial \boldsymbol{H}^e} = -\sqrt{\tfrac{3}{2}} A_3 \omega (1-\gamma_\infty)\exp(-\omega p)\,\boldsymbol{\upsilon} : \left[2\mu\mathbb{P} - \frac{\partial \boldsymbol{\beta}}{\partial \boldsymbol{H}^e}\right]. \tag{A6}$$

Taking the partial derivative with respect to $\boldsymbol{H}^e$ to $(A2)_2$ gives

$$\frac{\partial \Delta\lambda_s}{\partial \boldsymbol{H}^e} = \sqrt{\tfrac{3}{2}} r\,\Delta\lambda_s / J_2(\boldsymbol{\beta})\,\boldsymbol{\upsilon}_\beta : \frac{\partial \boldsymbol{\beta}}{\partial \boldsymbol{H}^e}, \tag{A7}$$

with $\boldsymbol{\upsilon}_\beta = \boldsymbol{\beta}/\|\boldsymbol{\beta}\|$.

By taking the partial derivative with respect to $\boldsymbol{H}^e$ to equation $(A1)_2$, together with application of the above relations to the corresponding partial derivatives, and after lengthy calculations we come to

$$\frac{\partial \boldsymbol{\beta}}{\partial \boldsymbol{H}^e} = \mathbb{B}^{-1} : \mathbb{G}, \tag{A8}$$

with

$$\begin{aligned}
&\mathbb{B} = B_1\mathbb{I} + B_2\,\boldsymbol{\upsilon}\otimes\boldsymbol{\upsilon} + B_3\,\boldsymbol{\upsilon}_\beta\otimes\boldsymbol{\upsilon} + B_4\,\boldsymbol{\upsilon}_\beta\otimes\boldsymbol{\upsilon}_\beta,\\
&B_1 = 1 + C\Delta\lambda_p\,[J_2^{-1}(\boldsymbol{S}-\boldsymbol{\beta}) + \gamma(p)/a] + d\Delta\lambda_s J_2^{-1}(\boldsymbol{\beta}),\\
&B_2 = C[A_3 - \Delta\lambda_p J_2^{-1}(\boldsymbol{S}-\boldsymbol{\beta})],\\
&B_3 = C A_3 J_2(\boldsymbol{\beta})/a\left[(\Delta\lambda_p\omega - 1)\gamma(p) - \omega\gamma_\infty\Delta\lambda_p\right],\\
&B_4 = d\Delta\lambda_s J_2^{-1}(\boldsymbol{\beta})(r-1).
\end{aligned} \tag{A9}$$

and

$$\begin{aligned}
&\mathbb{G} = G_1\mathbb{P} + G_2\,\boldsymbol{\upsilon}\otimes\boldsymbol{\upsilon} + G_3\,\boldsymbol{\upsilon}_\beta\otimes\boldsymbol{\upsilon},\\
&G_1 = 2\mu C\Delta\lambda_p J_2^{-1}(\boldsymbol{S}-\boldsymbol{\beta}),\\
&G_2 = 2\mu C\left[A_3 - \Delta\lambda_p J_2^{-1}(\boldsymbol{S}-\boldsymbol{\beta})\right],\\
&G_3 = 2\mu C A_3 J_2(\boldsymbol{\beta})/a\left[(\Delta\lambda_p\omega - 1)\gamma(p) - \omega\gamma_\infty\Delta\lambda_p\right] = 2\mu B_3.
\end{aligned} \tag{A10}$$

It can be easily seen that all the fourth-order tensors $\mathbb{B}$, $\mathbb{G}$ and $\partial\boldsymbol{\beta}/\partial\boldsymbol{H}^e$ fulfill the minor symmetries but do not satisfy the major symmetry. The reason for the latter comes from the recovery and

relaxation behavior included in the model. Taking the partial derivative with respect to $\boldsymbol{H}^e$ to equation $(A1)_1$ and exploiting the above related relations we obtain

$$\mathbb{K} = \frac{\partial \boldsymbol{H}^{e\,\mathrm{tr}}}{\partial \boldsymbol{H}^e} = \mathbb{I} + \tfrac{3}{2}\left[\Delta\lambda_p J_2^{-1}(\boldsymbol{S}-\boldsymbol{\beta})(\mathbb{I}-\boldsymbol{v}\otimes\boldsymbol{v}) + A_3\,\boldsymbol{v}\otimes\boldsymbol{v}\right] : \left[2\mu\mathbb{P} - \mathbb{B}^{-1} : \mathbb{G}\right]. \quad \text{(A11)}$$

Then,

$$\bar{\mathbb{C}}^{ep} = \frac{\partial \boldsymbol{T}}{\partial \boldsymbol{H}^{e\,\mathrm{tr}}} = \frac{\partial \boldsymbol{T}}{\partial \boldsymbol{H}^e} : \frac{\partial \boldsymbol{H}^e}{\partial \boldsymbol{H}^{e\,\mathrm{tr}}} = \mathbb{C} : \mathbb{K}^{-1}. \quad \text{(A12)}$$

Obviously, the algorithmic modulus tensor $\bar{\mathbb{C}}^{ep}$ also does not fulfill the major symmetry.

References

1. ABAQUS Manual: Getting Started with ABAQUS 6.4 (Hibbitt, Karlsson & Sorensen, Inc., 2003).
2. ABAQUS Theory Manual 5.8 (Hibbitt, Karlsson & Sorensen, Inc., 1998).
3. Arzt, M.; Brocks, W.; Mohr, R.; Qi, W.: User material routine for simulating anisothermal elasto-viscoplasticity and damage. Techincal Note GKSS/WMG/99/11.
4. Asaro, R.J.: Geometrical effects in the inhomogeneous deformation of ductile single crystals. Acta Metallurgica 27, (1979) 445-453.
5. Asaro, R.J.: Micromechanics of crystals and polycrystals. In: Advances Appl Mech, Vol. 23. Academic Press, New York, 1983.
6. Asaro, R.J.; J.R. Rice: Strain localization in ductile single crystals. J Mech Phys Solids 25, (1977) 309-338.
7. Betten, J.: Interpolation methods for tensor functions. In: Avula, X.J.R.(Ed): Mathematical Modelling in Science and Technology. Pergamon Press, New York, 1984, pp. 52-57.
8. Betten, J.: Generalization of nonlinear matherial laws found in experiments to multiaxial states of stress. Europ J Mech–A/Solids 8, (1989) 325-339 .
9. Betten, J.: Kontinuumsmechanik, 2. Aufl. Springer-Verlag, Berlin, 2001.
10. Betten, J.: Ceep Mechanics, 2nd Edition. Springer-Verlag, Berlin, 2005.
11. Chaboche, J.L.: Viscoplastic constitutive equations for the description of cyclic and anisotropic

behaviour of metals. In: Bull de l'Acad Polonaise des Sciences, Série Sc et Tech, 17th Polish Conf Mech Solids, Szczyrk, 1975, pp.33-41.

12. Chaboche, J.L.: Constitutive equations for cyclic plasticity and cyclic viscoplasticity. Int J Plasticity 5, (1989) 247-302.
13. Chaboche, J.L.: Cyclic viscoplastic constitutive equations, part I: A thermodynamically consistent formulation. ASME J Appl Mech 60, (1993) 813-821.
14. Chaboche, J.L.: Cyclic viscoplastic constitutive equations, part II: stored energy—comparison between models and experiments. ASME J Appl Mech 60, (1993) 822-828.
15. Chaboche, J.L.: Thermodynamic formulation of constitutive equations and application to the viscoplasticity and viscoelasticity of metals and polymers. Int J Solids Struct 34, (1997) 2239-2254.
16. Chaboche, J.L.; Jung, O.: Application of a kinematic hardening viscoplasticity model with thresholds to the residual stress relaxation. Int J Plasticity 13, (1998) 785-807.
17. Chaboche, J.L.; Rousselier, G.: On the plastic and viscoplastic constitutive equations—Part I: Rules developed with internal variable concept. ASME J Pressure Vessel Tech 34, (1983) 153-158.
18. Chaboche, J.L.; Rousselier, G.: On the plastic and viscoplastic constitutive equations—Part II: application of internal variable concepts to the 316 stainless steel. ASME J Pressure Vessel Tech 34, (1983) 159-164.
19. Fitzgerald, J.E.: A tensorial Hencky measure of strain and strain rate for finite deformations. J Appl Phys 51, (1980) 5111-5115.
20. Lehmann, Th.; Guo, Z.H.; Liang, H.Y.: The conjugacy bewteen Cauchy stress and logarithm of the left stretch tensor. Europ J Mech A/Solids 10, (1991) 395-404.
21. Lemaitre, J.; Chaboche, J.L.: Mechanics of Solids Materials. Cambridge University Press, 1990.
22. Lin, R.C.: Viscoelastic and elastic-viscoelastic-elastoplastic constitutive characterizations of polymers at finite strains: theoretical and numerical aspects. PhD Thesis, University of the Federal Armed Forces Hamburg, 2002.

23. Lin, R.C.: Numerical study of consistency of rate constitutive equations with elasticity at finite deformation. Int J Num Methods Engrg 55, (2002) 1053-1077.
24. Lin, R.C.: Analytical stress solutions of a closed deformation path with stretching and shearing using the hypoelastic formulations, Europ J Mech A/Solids 22, (2003) 443-461.
25. Lin, R.C.; Schomburg, U.: A finite elastic-viscoelastic-elastoplastic material law with damage: theoretical and numerical aspects. Comput Methods Appl Mech Engrg 192, (2003) 1591-1627.
26. Lin, R.C.; Brocks, W.: On a finite viscoplastic theory based on a new internal dissipation inequality. Int J Plasticity 20, (2004) 1281-1311.
27. Lin, R.C.; Brocks, W.; Betten, J.: On internal dissipation inequalities and finite strain inelastic constitutive laws: theoretical and numerical comparisons. Accepted for publication in Int J Plasticity.
28. Lion, A.: A physically based method to represent the thermo-mechanical behaviour of elastomers. Acta Mechanica 123, (1997a) 1-25.
29. Miehe, C.: A constitutive frame of elastoplasticity at large strains based on the notation of a plastic metric. Int J Solids Struct 35, (1998) 3859-3897.
30. Olschewski, J.; Sievert, R.; Meersmann, J; Ziebs, J.: Selection, cablibration and verification of viscoplastic constitutive models used for advanced blading methodology. In: Bachelet E. et al. (Eds): High Temperature Materials for Power Engineering. Kluwer Academic Publishers, pp. 1051-1060, 1990.
31. Olschewski, J.; Sievert, R.; Bertram, A.: A comparison of the predictive capabilities of two unified constitutive models at elevated temperatures. In: Desai C.S. et al. (Eds): Constitutive laws for engineering materials, Proceedings of the Third International Conference on Constitutive Laws for Engineering Materials: Theory and Applications, New York, 1991.
32. Simo, J.C.: Algorithms for static and dynamic multiplicative plasticity that preserve the classical return mapping schemes of the infinitesimal theory. Comput Methods Appl Mech Engrg 99, (1992) 61-112.
33. Simo, J.C.: Numerical analysis and simulation of plasticity. In: Ciarlet, P.G.; Lions, J.L. (Eds): Handbook of Numerical Analyis Vol. IV. Elsevier Science, Amsterdam, 1998.

34. Simo, J.C.; Hughes, T.J.R.: Computational Inelasticity. Springer-Verlag, New York Inc., 1998.
35. Simo, J.C.; Miehe, C.: Associative coupled thermoplasticity at finite strains: formulation, numerical Analysis and implementation. Comput Methods Appl Mech Engrg 98, (1992) 41-104.
36. Simo, J.C.; Pister, K.S.: Remarks on rate constitutive equations for finite deformation problems: computational implicatons. Comput Methods Appl Mech Engrg 46, (1984) 201-215.
37. Xiao, H.; Bruhns, O.T.; Meyers, A.: On objective corotational rates and their defining spin tensors. Int J Solids Struc 35, (1998) 4001-4014.
38. Xiao, H.; Bruhns O.T.; Meyers, A.: Strain rates and material spins. J Elasticity 52, (1998) 1-41.